Available online at www.sciencedirect.com
ScienceDirect
Mathematics and Computers in Simulation xxx (xxxx) xxx
MATHEMATICS AND COMPUTERS IN SIMULATION
www.elsevier.com/locate/matcom

Original articles

Tool for optimization of sale and storage of energy in wind farms☆

Eloy Celades[a], Emilio Pérez[b], Néstor Aparicio[b], Ignacio Peñarrocha-Alós[b,*]

[a] GALT Automation, C. Bulgaria, nave 8B, 12006 Castelló de la Plana, Spain
[b] ESID – Universitat Jaume I, Av. Vicent Sos Baynat, s/n, 12071 Castelló de la Plana, Spain

Received 17 October 2022; received in revised form 23 February 2023; accepted 9 March 2023
Available online xxxx

Abstract

In this work we address the problem of energy management in a wind farm supported by an Energy Storage System (ESS) that operates in an electricity market with six intraday sessions and with penalty policies for imbalances between commitments and the energy really injected. We face it through a cascade of model predictive controllers that also require the design of predictors for wind and electricity market price forecasts. The master controller is executed synchronously with the market sessions and decides the commitments. The slave controller is executed each hour and decides the energy that should be sold to minimize the economical penalties if the commitment is not achievable. Finally, a real-time controller decides how to manage the energy storage in the ESS to sell the desired energy when possible. We use historical real data for the design and validation of the approach and show its benefits. The results show that the cascade structure helps to adequately adapt the energy committed in the intraday market. We also obtain the necessary prices on batteries so that their use is profitable.

Keywords: Dispatching optimization; Imbalance minimization; Electricity market; Wind forecast; Price forecast; Energy storage

1. Introduction

During the year 2021, and despite the pandemic and the supply shocks suffered, renewable energies have experienced another record in growth of power capacity. Furthermore, the conflict in Ukraine has made clearer than ever the importance of energy security and sovereignty, for which renewable energies also play a key role [19]. Indeed, solar and wind power provided more than 10% of the world's electricity for the first time ever. Regarding wind power in particular, an estimated 102 GW capacity was installed globally in 2021, making total global capacity to surpass 845 GW [19].

However, this growth in renewables is proving increasingly difficult due to the stochastic and intermittent nature inherent in this type of generation [10,12,23]. If not properly addressed, the variations in the power generated by renewable sources can result in deviations in network voltage and frequency [21]. Furthermore, other technical challenges such as grid interconnection, power quality, reliability, protection, generation dispatch, and control also

☆ Funding: This work was supported by the Spanish State Research Agency under grants PID2020-112943RB-I00, PID2021-125634OB-I00 and TED2021-130120B-C22, ERDF, EU; and the Universitat Jaume I through project number UJI-B2021-35.
* Corresponding author.
E-mail addresses: ecelades@galtautomation.com (E. Celades), pereze@uji.es (E. Pérez), aparicio@uji.es (N. Aparicio), ipenarro@uji.es (I. Peñarrocha-Alós).

https://doi.org/10.1016/j.matcom.2023.03.010

arise [22]. Moreover, given that electricity transport and distribution infrastructures are not updated at such a quick pace as the renewable technologies are increasing their share of the electric production mix, transmission system operators (TSO) will not be able to rely on a higher interconnection capacity that would allow further power exchanges among control areas, which is a traditional way to balance the system. Instead, alternative ways of providing flexibility, mainly based on energy storage systems (ESS), are being proposed and developed [8,26].

In this sense, plenty of works study how the introduction of ESS allows renewable energy sources to maintain the injection of power committed to the electricity markets, granting precise production commitments by periods [1–4,11,14,17].

There are also several works in the literature that address the control of wind farm with ESS in particular. For instance, in [22] authors propose a strategy to use the ESS to smooth the power output of the wind farm. In a second work [21], by most of the authors of the previous one, a different smoothing strategy is introduced, based on optimal control. The proposed algorithm tries to follow a reference given as the forecast power of the wind farm for the next hour, which is assumed to be known with a constant error. Authors in [24] also present a strategy for minimizing power fluctuations, considering the use of batteries together with a hydrogen conversion system, introduced to overcome the limitations of the former. However, none of these proposals considers direct participation in electricity markets or uses a realistic forecast.

Regarding the participation of wind farms with ESS in electricity markets, some contributions have been made in recent years. In [27] the authors introduce a similar approach to the one proposed here, with two optimization stages, one for a daily market and one for a real-time market. However, their proposal lacks a strategy to minimize the penalties incurred for committing deviations from the power commitments. On the contrary, [6] focuses on maximizing the wind farm profits by minimizing deviations while also considering the cost of batteries degradation, but without considering the calculation of power commitments, which are assumed to be given. A different approach, based on reinforcement learning, is proposed in [25]. In that work, the authors consider the up/down reserve purchase, together with the ESS charge/discharge, to achieve an optimal revenue.

This paper proposes a tool which takes advantage of the flexibility provided by an ESS to implement an optimization-based strategy for maximizing the benefits of a wind farm participating in daily and intraday electricity markets with a 48 h horizon. This strategy makes use of forecasting techniques for wind speed and electricity prices. Furthermore, the proposed approach also addresses the minimization of future penalties, incurred because of deviations from power commitments, with a second optimization layer. This second optimization has a 6 h horizon which allows the use of updated and more precise short-term wind and price forecasts. The proposed strategies are analyzed for the Iberian electricity market (MIBEL) although they can be straightforwardly transposed to the European Cross Border Intraday Market (XBID) [15].

Furthermore, this work also analyses the economic feasibility of the inclusion of the ESS in the described framework by determining the maximum price, in €/kWh, which would make the strategy profitable. Although the results are valid for any type of ESS, lithium-ion (Li-ion) batteries in particular are considered due to the tenfold downward trend in per kilowatt hour cost experienced by commercial battery packs in the last 10 years [5,18].

The structure of the paper is as follows. First, the statement of the problem will be presented. In Section 3, the five parts that make up the proposed control tool will be described. Section 4 is devoted to introducing the results and, finally, some conclusions will be drawn.

2. Problem statement

In this work we consider the problem of maximizing the income in a wind farm supported by an ESS that operates in a market with several sessions along the day. First, the different agents make their offers in a daily market, which is closed by noon of the day before delivery. Therefore, at that time the agents know their production commitment for each hour of the delivery day. Later, these commitments can be adapted in the intraday market sessions. Furthermore, the market has a penalty policy for productions that do not fit the previously committed values. In that sense, the wind farm must communicate the production commitment several times a day, and, finally, it must decide how to operate the plant in real-time in terms of the amount of energy to be fed to the grid and stored in or delivered by the ESS, in order to maximize the incomes under the uncertainty of the wind that finally is available at each period of time. The operation of the plant must take into account the fact that the committed values may not be feasibly affordable with the available power and stored energy in the ESS.

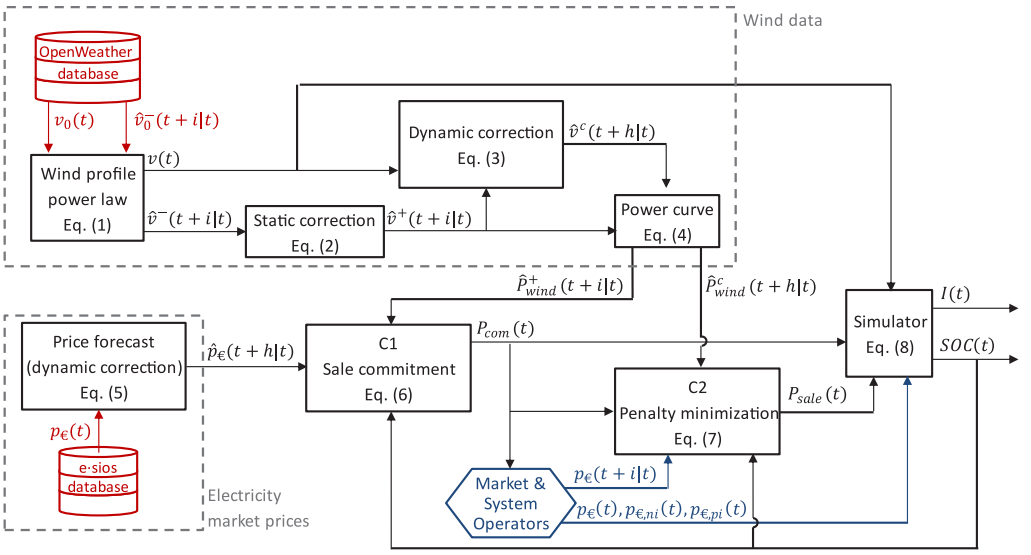

Fig. 1. Block diagram of the proposed tool.

The use of an ESS can help the wind farm to (i) feed the grid in the periods with higher electricity prices in order to maximize the benefit, and (ii) to avoid penalties when the available wind power does not adjust to the power that had previously been committed to inject.

To face this problem, we assume that we have access to databases that store values of past wind speed measurements and that offer some wind forecast, which may have some systematic errors, and where their policy to forecast and to update those values is not known for the final user. We also assume that we have access to the historical data of prices of the market where we are operating.

With these scenarios, the problem is how to develop a control scheme that decides the future commitments to be communicated to the market operator, the real energy that is finally fed to the grid, and how to manage the charge and discharge of the ESS. These decisions must be taken considering the different physical limitations (in terms of rated powers and ESS capacity) and taking into account the time varying scenario in terms of available historical or future data at each instant of time, and the different instants of time along day where the commitments must be done.

In this work, we particularize our problem in the operation of a wind farm near Valencia, in the east of Spain, and assume that it is supported with an ESS and connected through a substation. The wind farm is made up of a total of 23 2.1 MW wind turbines with a tower height of 114 m.

3. Proposed control tool

In order to address the stated problem, we propose, in general terms, a cascade of controllers that are based on predictors and follow a Model Predictive Control strategy. The designed control tool can be divided into a total of five parts depending on its main function, as depicted in the block diagram shown in Fig. 1, which are:

- Wind data (measurements and forecasts).
- Electricity market prices (actual and forecast).
- Controller C1. Energy sale commitment calculation.
- Controller C2. Imbalance penalty minimization.
- Simulator.

The list of variables used in the control tool are shown in Table 1.

Table 1
List of variables used in the control tool.

Variable	Description	Unit
C_{bat}	Battery capacity	MWh
$I(t)$	Resulting income	€
$P_{com}(t)$	Power commitment of each hour	MW
$P_{sale}(t)$	Power finally sold each hour	MW
$\hat{P}^{+}_{wind}(t+i\|t)$	Power that would be generated with speed $\hat{v}^{+}(t+i\|t)$	MW
$\hat{P}^{c}_{wind}(t+h\|t)$	Power that would be generated with speed $\hat{v}^{c}(t+h\|t)$	MW
$p_{€}(t)$	Electricity price	€/MWh
$p_{€,ni}(t)$	Negative imbalance price	€/MWh
$p_{€,pi}(t)$	Positive imbalance price	€/MWh
$p_{€}(t+i\|t)$	Already known prices of the active market session	€/MWh
$\hat{p}_{€}(t+h\|t)$	Calculated market price forecasts	€/MWh
$SOC(t)$	State of charge	%
$v_0(t)$	Average of the measured wind speed stored in the database	m/s
$\hat{v}_0^{-}(t+i\|t)$	Wind speed forecasts offered by the database	m/s
$v(t)$	$v_0(t)$ adapted to the height of the wind turbine	m/s
$\hat{v}^{-}(t+i\|t)$	$v_0^{-}(t+h\|t)$ adapted to the height of the wind turbine	m/s
$\hat{v}^{+}(t+i\|t)$	Static correction of $\hat{v}^{-}(t+i\|t)$	m/s
$\hat{v}^{c}(t+h\|t)$	Wind speed predictor	m/s
δ_t	Sampling period (one hour)	h
η_c	Battery efficiency for charge	%
η_d	Battery efficiency for discharge	%

3.1. Wind data

This block is responsible for providing, on the one hand, the real wind measurements and, on the other hand, the wind generation forecast necessary in both controllers.

We split this block in several subsystems, where the main functions are:

- Access to a wind speed database that includes both historical values and forecasts.
- Height adaptation of the wind speed.
- Static correction to address the systematic error between the forecasts and finally measured wind speed in the database.
- Dynamic prediction to improve the forecasts with respect to the ones provided in the database and in order to achieve larger horizons that the ones available in the database.
- Wind speed to power conversion.

In this work we use the OpenWeatherMap One Call API (application programming interface) [16] to obtain historical data and initial forecasts. This API shares historical values of hourly measured wind data in a given location and at the height of the instrument measurement ($h_{meas} = 10$ m) up to the hour of access, and also offers hourly forecasts of the wind speed values with a 48-hour horizon. In this work we use t to specify time index, and we use discrete time indices.[1] In that sense, t refers to the hour in absolute terms, i.e., extracting the absolute number of accumulated hours in an absolute time index as Unix timestamp. Let us call $v_0(t)$ the average value of wind speed between $t-1$ and t that is measured and stored in the database at t, and available since that time t. Let us call $\hat{v}_0^{-}(t+i|t)$ $(i = 1, \ldots, 48)$ the offered forecast values in the database at time t for the next 48 h to come. The API only offers the most updated forecasts, i.e., when you access to the database at $t+1$, you will find the forecasts $\hat{v}_0^{-}(t+i|t+1)$ $(i = 2, \ldots, 48)$ that do not necessarily match the previously forecasts $\hat{v}_0^{-}(t+i|t)$ $(i = 2, \ldots, 48)$ that were found at t and that cannot be found when you access at $t+1$ as they are replaced by the newer forecasts $\hat{v}_0^{-}(t+i|t+1)$.

[1] Variable t denotes the absolute number of hours in Unix time. In this work, the sampling period for each of the estimations, forecasts and optimizations is one hour ($\delta_t = 1$). Therefore, t can also be seen as the discrete-time index, being an integer value. Expressions as $t-1$ or $t+1$ refer both to one sample before or after, or one hour before or after.

As our aim is to estimate available wind power, we first adapt all measurements and forecasts data of the aforementioned API to the height of the wind turbine tower, that is, $h_{top} = 114$ m. We use Hellman's power law for that height adaptation, which leads to the wind speed at the rotor through

$$v(t) = v_0(t)\left(\frac{h_{top}}{h_{meas}}\right)^{\alpha} \tag{1a}$$

$$\hat{v}^{-}(t+i|t) = \hat{v}_0^{-}(t+i|t)\left(\frac{h_{top}}{h_{meas}}\right)^{\alpha} \tag{1b}$$

where h_{top} refers to the height of the rotor (114 m), h_{meas} the height where the measurements are taken (10 m) and $\alpha = 0.15$ depends on the geographical surroundings of the wind farm location.

Then, we analyze the accuracy of the offered forecasts. In order to perform that analysis, we have automated hourly access to the database for 34 days (from 24/04/2021 to 27/05/2021). We have stored at each t (with $t = t_0, \ldots, t_0 + N$, with $N = 34 \cdot 24 = 816$ and t_0 the absolute Unix hour of the initialization date of data acquisition) the available wind measurement $v(t)$ and forecasts $\hat{v}^{-}(t+i|t)$ (after height adaptation through). In order to quantify the quality of the available forecasts we have compared the measurements with their different predictions, i.e., each $v(t+i)$ with all the possible predictions $\hat{v}^{-}(t+i|t)$ with $i = 1, \ldots, 48$, leading to an average wind speed error (bias) of 0.8 m/s, an average of the absolute error of 1.76 m/s, a maximum registered error of 9.58 m/s, and a standard deviation of 2.25 m/s. In this sense, a systematic error is found, probably due to the fact that this data source is not a predictor intended specifically for wind generation.

In order to overcome the systematic error inherent to the selected database, we propose to use a static correction through a second-degree polynomial function of the form

$$\hat{v}^{+}(t+i|t) = a + b\,\hat{v}^{-}(t+i|t) + c\,\hat{v}^{-}(t+i|t)^2 \tag{2}$$

where $\hat{v}^{+}(t+i|t)$ refers to the corrected forecast. In order to obtain the coefficients, we try to fit equation

$$v(t+i) = \begin{bmatrix} 1 & \hat{v}^{-}(t+i|t) & \hat{v}^{-}(t+i|t)^2 \end{bmatrix} \begin{bmatrix} a \\ b \\ c \end{bmatrix}$$

for $t = t_0 + i, \ldots, t_0 + N - i$ and $i = 1, \ldots, 48$ in the mean square sense. Then, using a least squares regression, we obtain the coefficients $a = 0.7232$, $b = 0.7034$ and $c = -0.0338$. With this we obtain an average wind speed error (bias) of 0.01 m/s, an average of the absolute error of 1.4 m/s, a maximum registered error of 7.1 m/s, and a standard deviation of 1.8 m/s, showing an improvement in the forecast values initially supplied from the database.

Once the inherent systematic forecast errors are corrected, we try to improve short-term forecasts used by controller C2 with the goal of avoiding penalties.

This controller needs wind speed forecasts for the next 6 h. A dynamic correction is applied to the forecast for the following 6 h by using a different predictor for each of the horizons (i.e., a bank of predictors). Each predictor estimates at instant t the future wind speed at the rotor height at a future instant $t+h$ as a function of $\hat{v}^{+}(t+h|t)$ (the wind speed predicted from the app, adapted by and corrected by (2)), as well as $v(t-j)$ (the registered wind speed at previous instants adapted by), and the wind speed that was estimated for that previous periods in previous forecasts (i.e., $\hat{v}^{+}(t-j|t-j)$, where $\hat{v}^{+}(t-j|t-j)$ refers to the newest forecast that is available, but where the instant of update in the API is unknown but before $t-j$). This leads to a set of 6 different predictors, one for each time horizon $h = 1, \ldots, 6$ as follows

$$\hat{v}^{c}(t+h|t) = a_h + b_h\hat{v}^{+}(t+h|t) + \sum_{j=1}^{6} c_{h,j}\hat{v}^{+}(t-j|t-j) + d_{h,j}v(t-j). \tag{3}$$

Note that h is used in this case for both pointing to a future instant of time and enumerating the used predictor from the set of predictors, while $t-j$ is used to point at an instant of time previous to the time of executing the prediction (at t). The coefficients a_h, b_h, $c_{h,j}$ and $d_{h,j}$ of the six predictors are obtained through a linear regression that tries to fit the corrected predictions with the measured data in a given time window in a mean square sense. In order to obtain the coefficients, we try to fit, in the mean square sense, equations

$$v(t+h) = \phi(t,h)\theta(h), \qquad h = 1, \ldots, 6$$

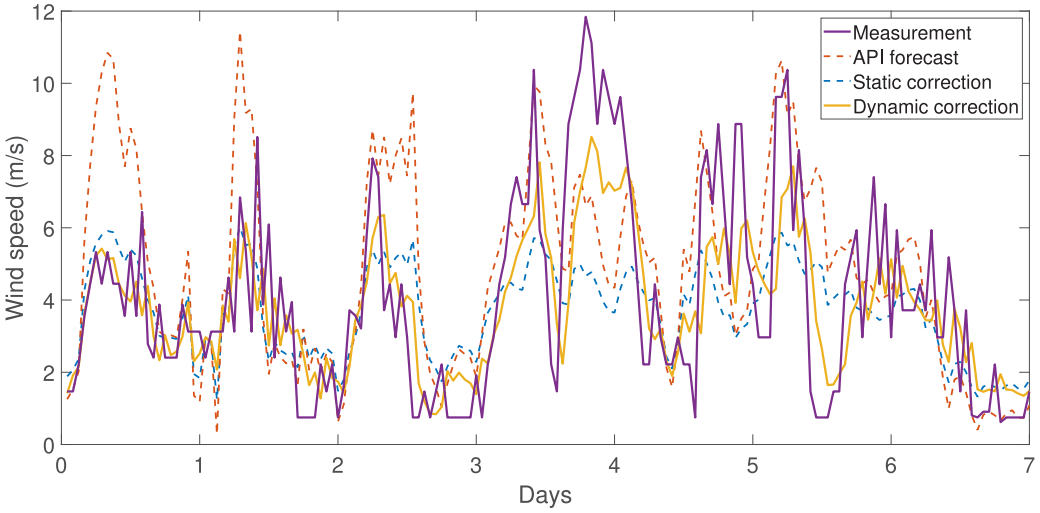

Fig. 2. Comparison between the measured wind data ($v(t)$), predictions coming from OpenWeatherMap ($\hat{v}^-(t|t-h)$) and after its correction ($\hat{v}^c(t|t-h)$), for horizon $h = 1$.

with

$$\phi(t,h) = \begin{bmatrix} 1 & \hat{v}^+(t+h|t) & \hat{v}^+(t-1|t-1) & \cdots & \hat{v}^+(t-6|t-6) & v(t-1) & \cdots & v(t-6) \end{bmatrix}$$

and

$$\theta(h)^T = \begin{bmatrix} a_h & b_h & c_{h,1} & \cdots & c_{h,6} & d_{h,1} & \cdots & d_{h,6} \end{bmatrix}$$

for $t = t_0 + 6, \ldots, t_0 + N - 6$ and $h = 1, \ldots, 6$.

The improvement in prediction can be seen in Fig. 2, where we can appreciate the forecast supplied by the API during a week for horizon $h = 1$ (i.e., using predictor number $h = 1$ from the set of 6 predictors), and its static and dynamic corrections (i.e., we are showing the wind values $\hat{v}^-(t|t-1)$, $\hat{v}^+(t|t-1)$ and $\hat{v}^c(t|t-1)$). We also show the wind that was finally measured (and known a posteriori) to see how the dynamic correction helps us in the short-term predictions.

We present in Table 2 different metrics for the wind forecast errors for the considered horizons (from $h = 1$ to 6 for $\hat{v}^-(t+h|t)$, $\hat{v}^+(t+h|t)$ and $\hat{v}^c(t+h|t)$), that are computed with the data set of 34 days with 24 real values $v_0(t)$ per day and 6 different forecasts $\hat{v}_0^-(t+h|t)$ given by the OpenWeatherMap tool for each hour. We present average values (denoted as $\mu(\cdot)$), average absolute values ($\mu(|\cdot|)$) maximum absolute values ($|\cdot|_{\max}$) and standard deviation ($\sigma(\cdot)$) for the errors in the provided forecast by the API (denoted as e^- and meaning $e^- \equiv v(t+h) - \hat{v}^-(t+h|t)$ for each horizon h), the errors after applying the static correction ($e^+ \equiv v(t+h) - \hat{v}^+(t+h|t)$), and after applying the dynamic one ($e^c \equiv v(t+h) - \hat{v}^c(t+h|t)$). As the parameters of the different correction approaches have been obtained through least squares, the standard deviation is the index that shows a better performance in all cases. We have also achieved an improvement of the errors in absolute terms for the dynamic correction for low horizons ($h = 1$ and $h = 2$), which will be profitable for the controller that tries to avoid penalties for not fulfilling the commitment (controller C2). The validation of this approach leads, for instance, to average absolute errors that go from 1.18 m/s (for $h = 1$) to 1.38 m/s (for $h = 6$). This dynamic correction leads to maximum prediction errors of 5.4 m/s and 7 m/s for low horizons ($h = 1$ and $h = 2$, respectively), showing an improvement with respect to the initial static correction (see Table 2).

Once this wind speed is obtained, we apply the power curve of a commercial wind turbine to obtain the generated power, that is,

$$P_{wind} = f(v). \tag{4}$$

Table 2
Metrics to assess wind forecasts errors (in m/s) for different horizons.

h	$\mu(e^-)$	$\mu(e^+)$	$\mu(e^c)$	$\mu(\lvert e^-\rvert)$	$\mu(\lvert e^+\rvert)$	$\mu(\lvert e^c\rvert)$	$\lvert e^-\rvert_{\max}$	$\lvert e^+\rvert_{\max}$	$\lvert e^c\rvert_{\max}$	$\sigma(e^-)$	$\sigma(e^+)$	$\sigma(e^c)$
1	−0.8044	0.0072	0.0647	1.7630	1.3925	1.1789	9.5798	7.1745	5.4082	2.2498	1.7933	1.5117
2	−0.8042	0.0088	0.0900	1.7638	1.3924	1.2814	9.5798	7.1745	7.0853	2.2510	1.7936	1.6570
3	−0.8063	0.0083	0.1018	1.7645	1.3935	1.3332	9.5798	7.1745	7.1492	2.2514	1.7945	1.7276
4	−0.8069	0.0095	0.1054	1.7661	1.3939	1.3613	9.5798	7.1745	7.1735	2.2526	1.7952	1.7600
5	−0.8115	0.0065	0.1078	1.7644	1.3925	1.3802	9.5798	7.1745	7.7222	2.2495	1.7940	1.7772
6	−0.8151	0.0048	0.1053	1.7636	1.3923	1.3835	9.5798	7.1745	7.6679	2.2482	1.7943	1.7848

Table 3
Intraday market session characteristics.

Intraday market	Gate closure	Horizon
Session 1	15:00	24 h Day D: 0:00–23:59
Session 2	17:50	28 h Day D–1: 20:00–23:59 Day D: 0:00–23:59
Session 3	21:50	24 h Day D: 0:00–23:59
Session 4	01:50	20 h Day D: 4:00–23:59
Session 5	04:50	17 h Day D: 7:00–23:59
Session 6	09:50	12 h Day D: 12:00–23:59

As the wind turbine is assumed to be under control, that function includes the fact that the generated power is limited to the rated power at high wind speeds. We compute $\hat{P}^{+}_{wind}(t+i|t)$ for controller C1 using $f(\hat{v}^{+}(t+i|t))$ and $\hat{P}^{c}_{wind}(t+i|t)$ for controller C2 using $f(\hat{v}^{c}(t+i|t))$, i.e.,

$$\hat{P}^{+}_{wind}(t+i|t) = f(\hat{v}^{+}(t+i|t)), \qquad i = 1,\ldots,48$$
$$\hat{P}^{c}_{wind}(t+h|t) = f(\hat{v}^{c}(t+h|t)), \qquad h = 1,\ldots,6$$

3.2. Electric market prices

This part of the tool is responsible for obtaining electricity market prices and processing them in order to obtain a forecast of the market prices for later use in both controllers.

The simulations of this work have been carried out for the Iberian electricity market, which is part of the European project called Price Coupling Regions (PCR), and that works as explained schematically in Fig. 3 and explained in the following.

The day-ahead spot market is the main market, where agents submit 24 hourly energy purchase and sale offers for the delivery day (denoted as day D) by 12:00 (gate closure) of the day before ($D-1$). Each offer consists of energy, in MWh, and prices, in €/MWh.

In addition, already within $D-1$ and during D, agents can adjust their contractual positions by purchasing and selling energy in the intraday market. This allows wind generators to reschedule their production with updated forecasts. Instead of being continuous, this market is divided into six sessions, shown in Table 3 and Fig. 3, where new market operations are agreed as the delivery day (D) progresses. Fig. 4 shows the prices that are fixed during the different sessions, where a dot indicates the instant of time from which those prices are applied, and the duration of the prices correspond to the Horizon indicated in Table 3, as well as the red bar indicated in Fig. 3. These prices are known at the times indicated as Gate closure in Table 3, and indicated with a green circle in Fig. 3.

Note that, as previously discussed, the purchase and sale bids in the day-ahead and intraday markets consist of two quantities: energy amount and minimum price to be accepted. However, in this work we omit the latter because the minimum acceptable price for the wind farm, as for other renewable sources, is always set to 0 in order to assure

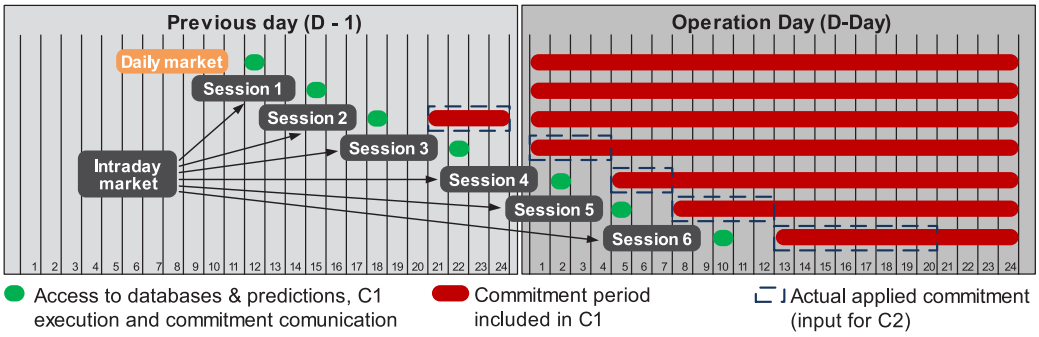

Fig. 3. Sequencing of day-ahead and intraday markets scheduling.

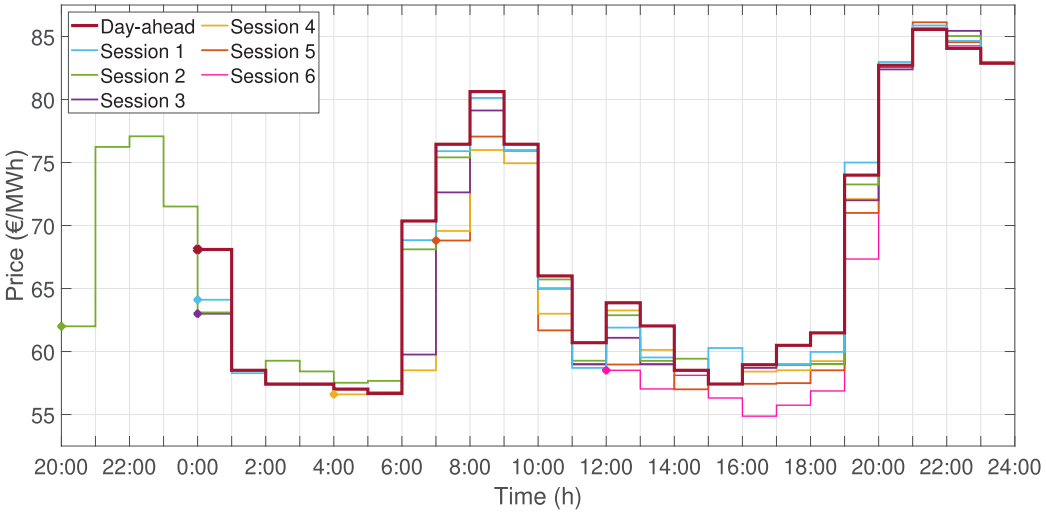

Fig. 4. Prices of day-ahead and intraday markets (24 May 2021).

the participation in the market at whichever price it closes, avoiding the opportunity cost of not generating when there is enough wind speed. Furthermore, the final market price is the result of bargaining. In this sense, the offers made by the wind farm could potentially change the market results. In this work, however, we consider that the total power of the wind farm is not high enough to affect the market result and, therefore, the wind farm is a price taker. In the literature there are different approaches for the market strategy of a wind farm when it is considered a price maker based, for instance, in game theory [20].

One of the problems faced by the algorithm to optimize the committed energy (controller C1) is that the price curves are not known at the moment when the commitment is made, since they are published after the gate closure.

For this reason, it is necessary to carry out a prediction of the market price curves, making use of historical price data that can be found on the e·sios website [9], which belongs to the Spanish TSO. For this prediction, more than the exact price for each hour, it stands out to know the hours in which the price reaches its maximum and its minimum, since the controller C1 is in charge of trying to discharge the ESS in the hours of higher prices (to sell the stored energy) and in charge of trying to send the wind acquired energy to the ESS in the hours of lower prices (to sell later this stored energy in higher prices periods), and thus maximize the benefit of the wind farm. In this sense, we can understand the ESS as a system to time-coupling the energy selling curve to the electricity market prices curve as much as possible.

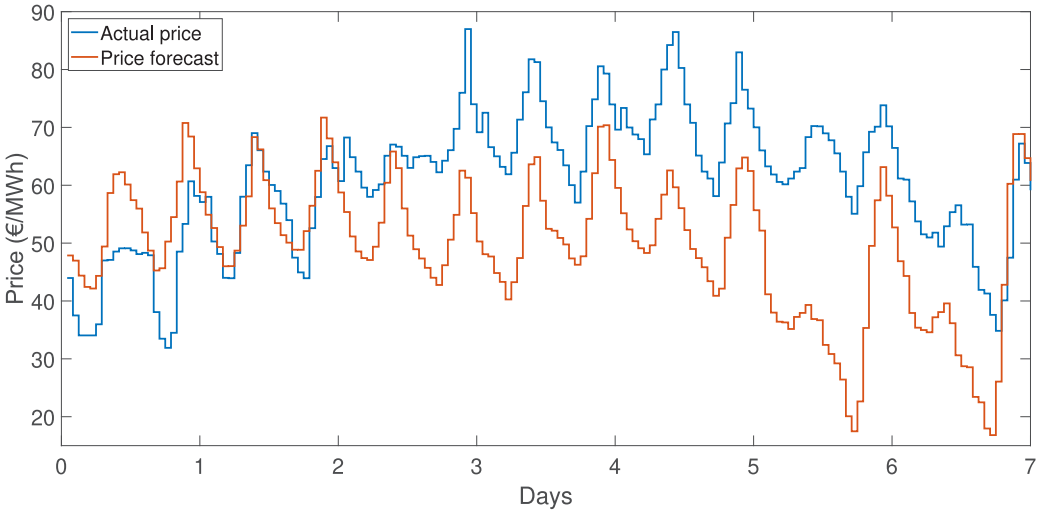

Fig. 5. Comparison of real market prices and the prediction for $h = 24$.

In order to predict the prices for the next 48 h, needed by controller C1, the following set of predictors ($h = 1, \ldots, 48$) is proposed

$$\hat{p}_{€}(t+h|t) = a_h + b_h\, p_{€}(t+h-48) + \sum_{j=1}^{4} c_{h,j}\, p_{€}(t+h-i\cdot 7\cdot 24) \tag{5}$$

where $\hat{p}_{€}(t+h|t)$ refers to the predicted price for instant $t+h$ computed at instant t using predictor numbered h from the set of available 48 predictors, $p_{€}(t)$ refers to the registered prices in e·sios for the daily market, and j is used to enumerate the past week whose recorded values are used for the prediction. Note that, at time t, all the terms in the right hand side refer to past known values: prices of the previous 4 weeks at the same time and week day that is being predicted (the time index $t+h-j\cdot 7\cdot 24$ with $j = 1, \ldots, 4$), and the price of the same time of the day 48 h ago (the time index $t+h-48$). Also note that for some instants of time $t+h$, the price may be already known and may be different depending on the market (day-ahead or intraday). However, even if values are known, we still make a prediction for those prices as our aim is to capture the price dynamics, not its exact value. The coefficients a_h, b_h and $c_{h,j}$ of each of the 48 predictors have been obtained using data from a 5-month time window and using least squares to fit the predicted prices to the finally registered ones, as detailed in the wind predictors. As an example, Fig. 5 shows the real prices and one of the 48 forecasts (for $h = 24$) during seven days.

In order to assess the goodness of the set of predictors $\hat{p}_{€}(t+h|t)$ in (5) for the different considered horizons (from $h = 1$ to 48) we use the data set of 5 months with 24 real values $p_{€}(t)$ per day. With these prediction errors we compute the mean absolute error leading to 12.7 €/MWh.

Although this error is not negligible, it can be seen how we capture the evolution throughout the day for most of the time (mainly the higher and lower peaks within a day), which helps the predictive controller to decide storing or injecting energy depending on the relative prices between periods.

The Iberian market also has a two-price system for settling imbalances. The imbalance price is the same as the market price for producers who do not contribute to the net imbalance of the system and a price with a penalty on the market price for those who do contribute. As an example, Fig. 6 shows the prices for a given day for the day-ahead market as well as positive and negative imbalances. Notice the negative imbalance price can never be lower than the day-ahead whereas the positive imbalance can never be higher. In this work we use notation $p_{€}(t)$ for normal price, and $p_{€,pi}(t)$ and $p_{€,ni}(t)$, for positive and negative imbalances, respectively. Therefore, from the previous statement it follows that

$$p_{€,pi}(t) \leq p_{€}(t) \leq p_{€,ni}(t).$$

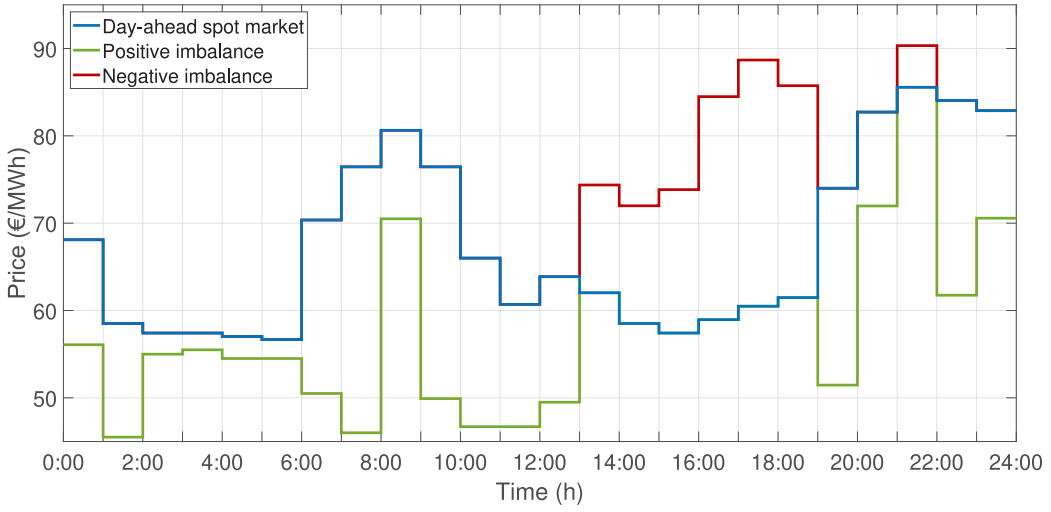

Fig. 6. Prices of the daily market and the positive and negative imbalances (24 May 2021).

We use the average value of those imbalance prices in relative terms with respect to the normal price as an estimation for the penalties in the imbalances, leading to $\hat{p}_{€,pi}(t) = 0.9\, p_€(t)$ and $\hat{p}_{€,ni}(t) = 1.1\, p_€(t)$. Thus the resulting income of a generator is its power commitment multiplied by the electricity price and, in the case of imbalance ($P_{sale} \neq P_{com}$) its either added its overproduction multiplied by the price of the positive imbalance is or subtracted its underproduction multiplied by the price of the negative imbalance.

3.3. C1 controller

This block takes as its starting point the wind forecasts given by the OpenWeatherMap API, with the previously introduced height adaptation, static correction ($\hat{v}^+(t+i|t)$) and translation to power units (with $\hat{P}^+_{wind}(t+i|t) = f(\hat{v}^+(t+i|t))$), the calculated market price forecasts ($\hat{p}_€(t+h|t)$), (both with a horizon up to 48 h) and the measured actual state of charge of the battery $SOC(t)$ in percentage of the battery capacity C_{bat}. The aim of this controller is to obtain market commitments for the energy generated, so that, depending on the battery charge level at each calculation instant, the pertinent computations will be carried out in order to obtain the amount of energy that is expected to be fed to the grid and the amount to be stored in (or taken from) the battery. This calculation will be made prior to the close of each electricity market (daily or intraday).

C1 controller consists of a model predictive controller which, at each instant it is executed, requires the following optimization problem to be solved:

$$\max_{P_{com},P^{C1}_{bat},SOC^{C1}} \sum_{i=1}^{48} (\hat{p}_€(t+i|t) \cdot P_{com}(t+i)) \tag{6}$$

subject to $SOC^{C1}(t) \equiv SOC(t)$

subject for $i = 1, \ldots, 48$ to

$$P_{com}(t+i) + P^{C1}_{bat}(t+i) \leq \hat{P}^+_{wind}(t+i|t)$$

$$SOC^{C1}(t+i) = \begin{cases} SOC^{C1}(t-1+i) + \frac{100\,\eta_c}{C_{bat}}\, P^{C1}_{bat}(t+i)\,\delta_t, & P^{C1}_{bat}(t+i) \geq 0 \\ SOC^{C1}(t-1+i) + \frac{100}{C_{bat}\,\eta_d}\, P^{C1}_{bat}(t+i)\,\delta_t, & P^{C1}_{bat}(t+i) < 0 \end{cases}$$

$$SOC^{C1}(t+48) = \frac{SOC_{\min} + SOC_{\max}}{2}$$

$$SOC_{\min} \leq SOC^{C1}(t+i) \leq SOC_{\max}$$

$$S_{TF} - P_{com}(t+i) \geq 0$$
$$-P_{bat_N} < P_{bat}^{C1}(t+i) < P_{bat_N}$$

where t is the time in which the calculations are made, $\hat{p}_{€}(t+i|t)$ is the market price forecast for hour $t+i$ calculated at instant t (that is obtained with predictor number $h=i$ in (5)), $P_{com}(t+i)$ is the power commitment during hour $t+i$, $P_{bat}^{C1}(t+i)$ is the charge or discharge power of the battery during the hour $t+i$, $\hat{P}_{wind}^{+}(t+i|t)$ is the wind power generation forecast during hour $t+i$, $SOC^{C1}(t+i)$ is the expected state of charge (SOC) at the end of hour $t+i$, C_{bat} is the capacity of the battery in Wh, $SOC_{\min}$ is the minimum SOC, $SOC_{\max}$ is the maximum SOC, S_{TF} is the transformer power rating, and P_{bat_N} is the nominal charging and discharging power of the battery. δ_t refers to the sampling period (one hour), and η_c and η_d refer to the battery efficiency for charge and discharge, respectively. The decision variables P_{com}, P_{bat}^{C1}, SOC^{C1} must be understood as the set of variables $\{P_{com}(t+i)\}$, $\{P_{bat}(t+i)\}$, $\{SOC^{C1}(t+i)\}$ with $i=1,\ldots,48$, plus $SOC^{C1}(t)$ that is used just for coherence in the notation (and is equal to the measured $SOC(t)$).

Note that this algorithm is executed during the periods indicated with a green circle in Fig. 3, i.e., a total of seven times during the day. Therefore, for each of the sessions, we must understand that we send to the market operator the commitments subset $\{P_{com}(t+i)\}$ where $t+i$ includes the periods of time indicated with a red bar in Fig. 3 for each of the sessions and indicated as $P_{com}(t)$ in Fig. 1.

Note also that we have chosen a horizon of 48 h although the applied values will be only a subset of the computed values, as the market requires updates in different sessions. However, we use this horizon to prevent the system of further high deviations of wind or prices, and in order to set a long-term desire of achieving an intermediate SOC in the battery after 48 h of the computation. This constraint prevents the algorithm from falling in extreme situations such as trying to sell all the stored energy in the battery at the end of the horizon.

The proposed optimization problem is non-linear due to the expression of SOC update, which changes depending on the sign of the power (charge or discharge process during the period). This kind of non-linearity can be addressed as a Sequential Least Square Program (SLSQP), for which there are efficient solvers available in Python [13], used in this work for the implementation.

With the assumption of a unitary battery efficiency for both charge and discharge, the SOC update equation reduces to

$$SOC^{C1}(t+i) = SOC^{C1}(t-1+i) + \frac{100}{C_{bat}} P_{bat}^{C1}(t+i)\,\delta_t$$

and, with this, problem (6) can be formulated as a Linear Program (LP) [7], for which there are also many available solvers in Python.

Furthermore, problem (6) can also be reformulated as a Linear Program even with non-unitary efficiency by defining two different power sequences (charging and discharging) and taking advantage of the fact that, because of the formulation of the problem itself, one of the two values will always be zero. Details are omitted here for brevity but a very similar strategy can be found in [17].

3.4. C2 controller

This second controller is responsible for calculating the charge or discharge of energy that the battery will perform for the next hour. This way, this controller is the one that decides the amount of energy that is in fact sold and the amount that goes to the battery at each hourly period. The goal of this controller, when deciding how to act in the wind farm, is to overcome previous prediction errors and, thus, wrong decisions (commitments previously given to the market operator during the computation of C1). In that sense, this controller uses a lower time horizon (6 h), and it is executed periodically each hour.

To do this, the controller will take as its starting point the wind forecasts together with the measurement records for each of the last 6 h and it will use them to make a dynamic forecast correction for the following 6 h, as explained in Section 3.1. This will be used with the turbine manufacturer equation to calculate a new generation forecast of the wind farm which will be compared with the commitment previously given by C1 controller (P_{com}) and the measured SOC at the instant of calculation, i.e. $SOC(t)$. In this way, it is calculated a new sequence of power values, P_{sale}, which is intended to minimize the penalties due to deviations between the expected and actual generation. If the wind and prices predictions used during the execution of C1 fit the real values, the output of

this controller P_{sale} will keep the previously computed target values for P_{com}. If that is not the case, this controller considers the cost of imbalances to decide the optimal deviation from P_{com} that assures the higher profit.

In Fig. 3 we appreciate with a black square the commitments P_{com} that act as an input for C2 controller depending on the hour of the day when it is executed. The following optimization problem is proposed for that purpose

$$\max_{P_{sale},P_{bat}^{C2},SOC^{C2}} \sum_{i=1}^{6} (p_{€}(t+i|t)\cdot P_{com}(t+i)+\pi(t+i)\cdot d(t+i)) \tag{7}$$

subject to $SOC^{C2}(t) \equiv SOC(t)$

subject for $i = 1,\ldots,6$ to

$$d(t+i) = P_{sale}(t+i) - P_{com}(t+i)$$

$$\pi(t+i) = \begin{cases} \hat{p}_{€,pi}(t+i),\ d(t+i) > 0 \\ \hat{p}_{€,ni}(t+i),\ d(t+i) < 0 \end{cases}$$

$$P_{sale}(t+i) + P_{bat}^{C2}(t+i) \le \hat{P}_{wind}^{c}(t+i|t)$$

$$SOC^{C2}(t+i) = \begin{cases} SOC^{C2}(t-1+i) + \frac{100\,\eta_c}{C_{bat}} P_{bat}^{C2}(t+i)\,\delta_t, & P_{bat}^{C2}(t+i) \ge 0 \\ SOC^{C2}(t-1+i) + \frac{100}{C_{bat}\,\eta_d} P_{bat}^{C2}(t+i)\,\delta_t, & P_{bat}^{C2}(t+i) < 0 \end{cases}$$

$$SOC_{\min} \le SOC^{C2}(t+i) \le SOC_{\max}$$

$$S_{TF} - P_{sale}(t+i) \ge 0$$

$$-P_{bat_N} < P_{bat}^{C2}(t+i) < P_{bat_N}$$

where $P_{sale}(t+i)$ is the decided sale to the market at each time, $p_{€}(t+i|t)$ are the already known prices for the active session in which controller C2 is being executed, $\hat{P}_{wind}^{c}(t+i|t)$ is the wind power generation forecast during hour $t+i$ that makes use of the dynamic correction ($\hat{P}_{wind}^{c}(t+i|t)$ must be understood as the prediction $\hat{P}_{wind}^{c}(t+h|t)$ using predictor number $h = i$ in (3) to generate the wind speed forecasts that generates that power value). Value $d(t)$ refers to the deviation between commitment and the injected power, and $\pi(t)$ is the estimated penalty cost that may be different depending on the sign of the deviation (with costs $\hat{p}_{€,pi}(t)$ and $\hat{p}_{€,ni}(t)$, as explained in Section 3.2). The decision variables P_{sale}, P_{bat}^{C2}, SOC^{C2} must be understood as the set of variables $\{P_{sale}(t+i)\}$, $\{P_{bat}(t+i)\}$, $\{SOC^{C2}(t+i)\}$ with $i = 1,\ldots,6$, plus $SOC^{C2}(t)$ that is used just for coherence in the notation (and is equal to the measured $SOC(t)$). From this set of values, we must understand that we finally only apply the value $P_{sale}(t+1)$, as a moving horizon strategy is applied. The output of this controller fits the real-time control of the wind farm included in the simulator block in Fig. 1, where this C2 controller output is denoted as $P_{sale}(t)$.

In this case, because of the non-linearity of the penalty cost function π and the consideration of the charge and discharge efficiency, we have again a non-linear optimization problem that can be formulated as a Sequential Least Square Program, or, analogously to Section 3.3, it can be translated into a Linear Program using the same ideas as in [17].

In this work we have used SLSQP to solve the above presented optimization problems, and each problem (at each sampling time) is solved in less than one second for the selected time horizons.

3.5. Simulator

This block is in charge of performing the calculations of the energy fed to the grid and updating the SOC assuming that the wind farm is operating with a wind equal to the measured one (after applying Hellman's law). In this sense, the block does not correspond to any specific control algorithm, but this update is carried out during the execution of the algorithms of both controllers to assess the proposal in a simulation framework and in order to achieve a realistic situation in which the decided power values to sell or store may in fact be unfeasible and, thus, a correction in the time of application must be done. In that sense, in the simulator, the injected P_{sale} or stored P_{bat} energy are modified with respect to the one decided in the controller C2. We call the finally applied values P_{sale}^{app} and P_{bat}^{app}. The correction will try to fit the finally injected power to the one that was decided to sell (P_{sale}) in C2 as far as the available wind power and charge of the battery allows it.

The simulation and correction algorithm works as follows. At instant t the simulator is in charge of updating the real value for the battery $SOC(t)$ and it has as inputs the values for power injection during t decided in C2 at $t-1$ (i.e. $P_{sale}(t)$), the real available wind power by means of $v(t)$ and Hellman's law, leading to $P_{wind}(t)$, the committed power for that period decided in controller C1 ($P_{com}(t)$, used for the computation of the real income), and the real electricity prices $p_{€}(t)$, $p_{€,pi}(t)$ and $p_{€,ni}(t)$ (see Fig. 1).

In this block we first compute the decision for the battery power injection or absorption to be applied (P_{bat}^{app}) and the power injection to the grid (P_{sale}^{app}). Then, we update the SOC of the battery with P_{bat}^{app} and compute the income with P_{sale}^{app}. In the following we detail those computations.

First, the actual room for battery charge or discharge is computed as

$$P_{bat,\max}(t) = min\left(\frac{C_{bat}}{100\,\eta_c\,\delta_t}(SOC_{\max} - SOC(t-1)),\, P_{bat_N}\right), \tag{8a}$$

and

$$P_{bat,\min}(t) = max\left(\frac{C_{bat}\,\eta_d}{100\,\delta_t}(SOC_{\min} - SOC(t-1)),\, -P_{bat_N}\right), \tag{8b}$$

respectively, where the available room as well as the nominal power value for the battery have been used for both positive and negative limits.

Then, the required use of battery to fulfill the desired power injection to the grid P_{sale} is computed as

$$P_{bat,req}(t) = P_{wind}(t) - P_{sale}(t). \tag{8c}$$

With the required battery use and its limits, the power that is ultimately injected into or extracted from the battery is computed as

$$P_{bat}^{app}(t) = \begin{cases} P_{bat,\min}(t), & P_{bat,req}(t) \le P_{bat,\min}(t), \\ P_{bat,req}(t), & P_{bat,\min}(t) < P_{bat,req}(t) < P_{bat,\max}(t), \\ P_{bat,\max}(t), & P_{bat,req}(t) \ge P_{bat,\max}(t). \end{cases} \tag{8d}$$

Here, if the battery has room for the required energy injection or absorption, the required power is the applied one, if not, we apply the maximum or minimum possible value (depending on the sign of $P_{bat,req}$). The final sale for power injection is given by

$$P_{sale}^{app}(t) = \begin{cases} P_{wind}(t) - P_{bat,\min}(t), & P_{bat,req}(t) \le P_{bat,\min}(t), \\ P_{sale}(t), & P_{bat,\min}(t) < P_{bat,req}(t) < P_{bat,\max}(t), \\ P_{wind}(t) - P_{bat,\max}(t), & P_{bat,req}(t) \ge P_{bat,\max}(t), \end{cases} \tag{8e}$$

that is, a value that depends on the available wind power and the power interchange with the battery.

Finally, with the previous decided values, the SOC is updated as

$$SOC(t) = \begin{cases} SOC(t-1) + \frac{100\,\eta_c}{C_{bat}}\,P_{bat}^{app}(t)\,\delta_t, & P_{bat}^{app}(t) \ge 0 \\ SOC(t-1) + \frac{100}{C_{bat}\,\eta_d}\,P_{bat}^{app}(t)\,\delta_t, & P_{bat}^{app}(t) < 0 \end{cases} \tag{8f}$$

and the resulting income $I(t)$ during hour t is computed as

$$I(t) = \begin{cases} \left[p_{€}(t)P_{com}(t) + p_{€,ni}(t)(P_{sale}^{app}(t) - P_{com}(t))\right]\delta_t, & P_{sale}^{app}(t) < P_{com}(t), \\ \left[p_{€}(t)P_{sale}^{app}(t)\right]\delta_t, & P_{sale}^{app}(t) = P_{com}(t), \\ \left[p_{€}(t)P_{com}(t) + p_{€,pi}(t)(P_{sale}^{app}(t) - P_{com}(t))\right]\delta_t, & P_{sale}^{app}(t) > P_{com}(t), \end{cases} \tag{8g}$$

where the penalties have been taken into account.

4. Results

In this section we present the results of applying the control strategy to the given wind farm for 37 days, between 21/05/2021 and 26/06/2021, when using a $C_{bat} = 48960$ kWh battery with a nominal power of 24 MW for a 48.3 MW wind farm. We propose the use of a battery that assures a 20-year lifespan (according to manufacturers), which

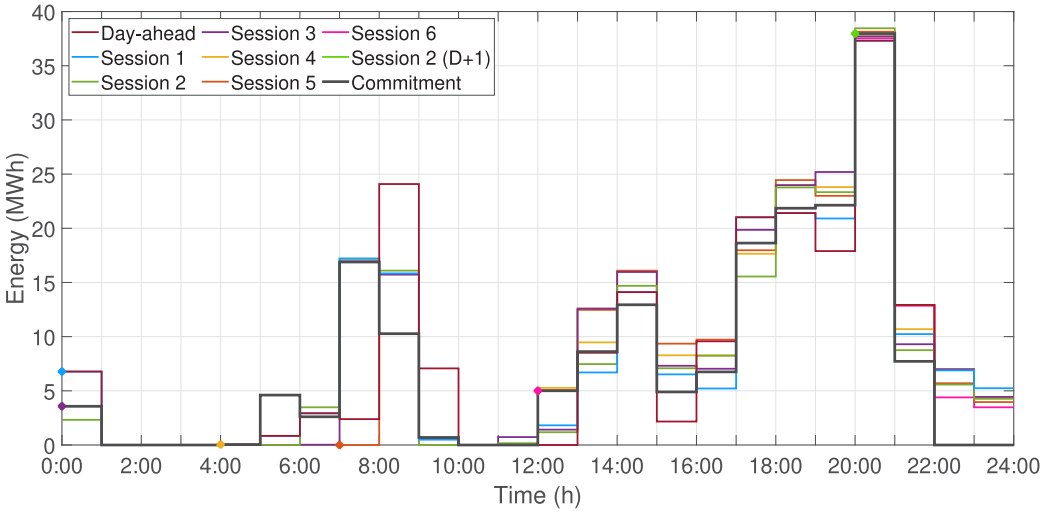

Fig. 7. Energy commitment with battery (14 June 2021).

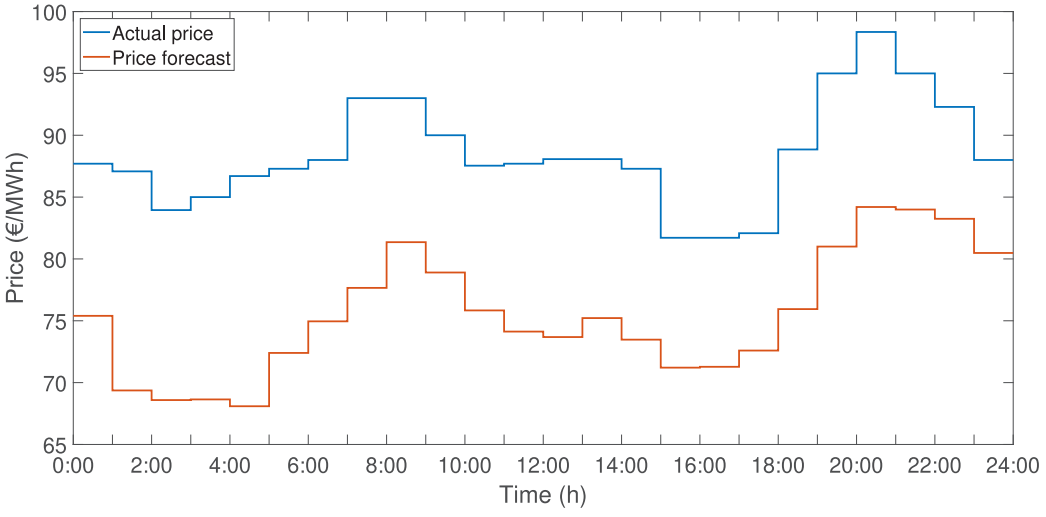

Fig. 8. Actual and predicted daily market prices (14 June 2021).

implies using states of charge between $SOC_{\min} = 20\%$ and $SOC_{\max} = 80\%$ with respect to the capacity C_{bat}. That means that the battery can store the equivalent of 0.6 h of the generation of the wind farm at its rated power. For the numerical example we also neglect the effect of the charging and discharging efficiencies ($\eta_c = \eta_d = 1$), which does not fundamentally change the results or the conclusions.

Both proposed controllers need the wind power and price forecasts given by the predictors introduced and assessed in previous sections of the work to support the theoretical explanations. In this section we omit the details about these forecasts to focus our attention on the coordinated work of the two controllers. The simulator is used to assess the behavior in terms of decisions about power commitment, sale or storage, and its influence in the reached income.

Figs. 7 and 8 show, respectively, the resulting commitment when applying C1 controller and the actual and forecast prices for the daily market. Fig. 9 shows the real wind speed for the same day, where we can appreciate that the available wind power and the evolution of market prices have different dynamics that must be faced through the use of the ESS. We see how in the period from 00:00 to 05:00 the controller decides to store energy to be able to sell it (discharging the battery) from 7:00, where the profits are higher, which demonstrates the effectiveness of

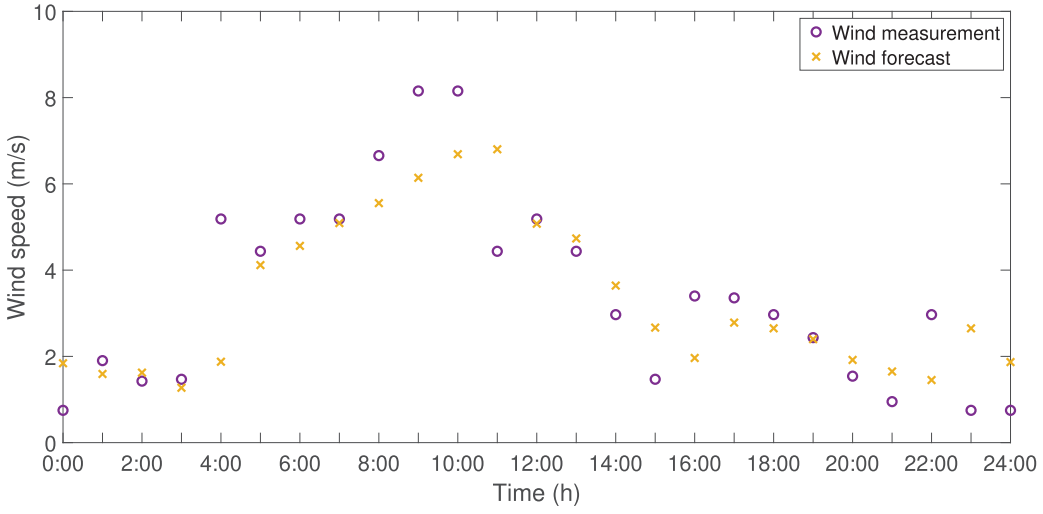

Fig. 9. Measured and predicted wind (14 June 2021).

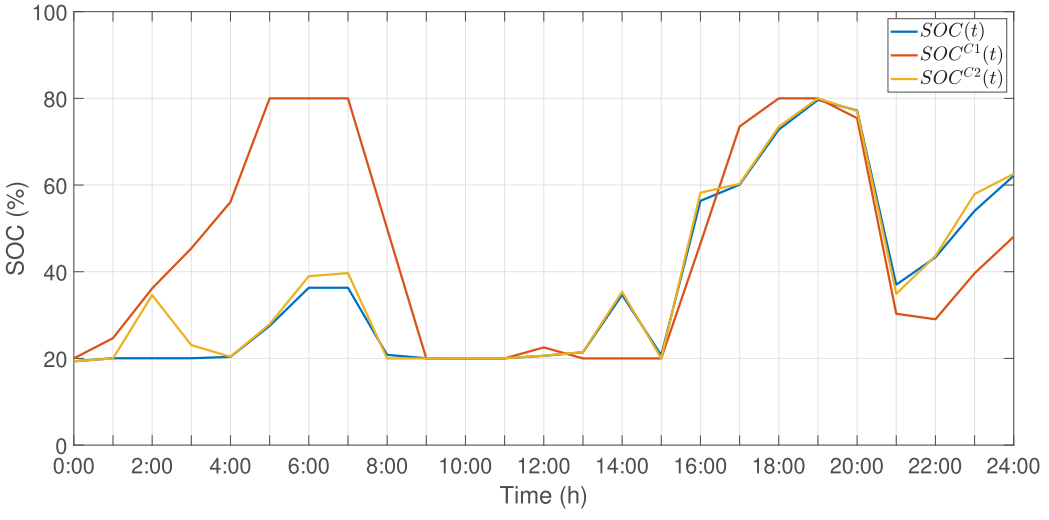

Fig. 10. Battery state of charge correction through controller C2.

the controller. In a comparable way, we see that at 15:00 the prices are lower and then the sale commitment is lower at that period, storing the energy available from the wind in order to sell it around 20:00, when the prices are higher.

In order to check the real effectiveness of the proposal, a simulation with the real measured wind is performed and assessed with the real price for that day. Fig. 10 shows the predictions for the battery state of charge during the optimization procedure in C1 (internal variable SOC^{C1} in C1), together with the estimated one to store internally in the computation of C2, i.e., SOC^{C2}, and the one finally obtained in the simulated system, (i.e., SOC), where the real measured wind has been used, showing the effectiveness of the two layers optimization. Here we appreciate that C2 takes into account a strong variation of the wind speed with respect to the initial forecasts used in C1), and, therefore, modifies the decision for power sell with respect to the initially committed values taking into account the penalties for power imbalance.

The proposed strategy has also been evaluated without the use of a battery to assess the benefits of including it (running the proposed algorithm with $SOC_{\min} = 50\%$ and $SOC_{\max} = 50\%$). The economic return in the simulated period without batteries has been 661 678 €, and with batteries, 691 215 €. In order to make this approach feasible with a return time of 20 years, the battery should have a price lower than 119.03 €/kWh.

The previous simulations have also been evaluated with a battery of 5100 kWh (equivalent to around 6 min capacity), leading to a benefit of 667 149 €. In that case, the price needed for the batteries to have a 20-year return would be 211.65 €/kWh.

5. Conclusions

In this work we have addressed the problem of controlling a wind farm with energy storage when facing an electricity market with time-varying prices in several daily and intraday sessions with penalty policies for power imbalance between previous commitments and injected energy. The control strategy decides the power commitment transmitted to the market operator, the amount of available wind energy that is injected to the grid, and the management of the ESS in terms of storing wind energy or selling stored energy.

The controller structure includes predictors for wind power and electricity prices, and a cascade of two model predictive controllers. The master controller is the one devoted to deciding the commitment that is transmitted to the market operator, and it is executed when the electricity market requires it in the different daily or intraday sessions. The slave controller is executed hourly and tries to maximize the benefit by means of using better estimations of the fore-coming wind speed and taking into account the penalties for power imbalance.

We have developed several predictors for wind power estimation taking into account the different needed horizons and the instants of time when they are needed. We have presented two optimization problems that must be solved at different instants of time and that use different inputs and outputs, and we have finally presented how to simulate the real behavior to assess the proposal.

With this, the tool has been proven useful to maximize the profit of a wind farm equipped with a battery. The adequate estimation achieved for both wind and electricity prices, especially in the short-term, together with a correct programming of both controllers, allows a good adjustment of energy commitments in the intraday market, to minimize penalties. However, the proposal shows that, even with the proposed structure, the use of batteries would only be beneficial for small capacities and with a price per kWh which has been estimated to be lower than what lithium-ion technology currently has. For this reason, alternative uses for batteries other than minimizing imbalances are being sought, such as the provision of ancillary services. Future research includes the use of batteries for these services, and design of predictors for power imbalance prices as well as for ancillary services prices.

References

[1] A.S. Awad, J.D. Fuller, T.H. El-Fouly, M.M. Salama, Impact of energy storage systems on electricity market equilibrium, IEEE Trans. Sustain. Energy 5 (3) (2014) 875–885, http://dx.doi.org/10.1109/TSTE.2014.2309661.

[2] T. Ayodele, A. Ogunjuyigbe, Mitigation of wind power intermittency: Storage technology approach, Renew. Sustain. Energy Rev. 44 (2015) 447–456, http://dx.doi.org/10.1016/j.rser.2014.12.034.

[3] H. Beltran, P. Ayuso, J. Cardo-Miota, J. Segarra-Tamarit, N. Aparicio, E. Pérez, Influence of the intraday electricity market structure on the degradation of li-ion batteries used to firm photovoltaic production, Energy Technol. 10 (2022) http://dx.doi.org/10.1002/ente.202100943.

[4] H. Beltran, E. Perez, N. Aparicio, P. Rodriguez, Daily Solar Energy Estimation for Minimizing Energy Storage Requirements in PV Power Plants, IEEE Trans. Sustain. Energy 4 (2) (2013) 474–481, http://dx.doi.org/10.1109/TSTE.2012.2206413.

[5] BloombergNEF, Electric vehicle outlook 2020, Technical Report, BloombergNEF, London, United Kingdom, 2020.

[6] R. Bourbon, S.U. Ngueveu, X. Roboam, B. Sareni, C. Turpin, D. Hernández-Torres, Energy management optimization of a smart wind power plant comparing heuristic and linear programming methods, Math. Comput. Simulation 158 (2019) 418–431, http://dx.doi.org/10.1016/j.matcom.2018.09.022.

[7] S. Boyd, S.P. Boyd, L. Vandenberghe, Convex Optimization, Cambridge University Press, 2004.

[8] Y. Dvorkin, R. Fernandez-Blanco, D.S. Kirschen, H. Pandžić, J.-P. Watson, C.A. Silva-Monroy, Ensuring profitability of energy storage, IEEE Trans. Power Syst. 32 (1) (2016) 611–623, http://dx.doi.org/10.1109/TPWRS.2016.2563259.

[9] e.sios, System operator information system, 2011, https://www.esios.ree.es/en. (Accessed on 30 January 2011).

[10] L. Hadjidemetriou, E. Kyriakides, F. Blaabjerg, A robust synchronization to enhance the power quality of renewable energy systems, IEEE Trans. Ind. Electron. 62 (8) (2015) 4858–4868, http://dx.doi.org/10.1109/TIE.2015.2397871.

[11] H.O.R. Howlader, O.B. Adewuyi, Y.Y. Hong, P. Mandal, A.M. Hemeida, T. Senjyu, Energy storage system analysis review for optimal unit commitment, Energies 13 (1) (2019) http://dx.doi.org/10.3390/en13010158.

[12] IRENA, Adapting market design to high shares of variable renewable energy, Technical Report, International Renewable Energy Agency (IRENA), Abu Dhabi, 2017, p. 168.

[13] D. Kraft, A software package for sequential quadratic programming, Forschungsbericht- Deutsche Forschungs- und Versuchsanstalt fur Luft- und Raumfahrt (1988).

[14] K. Maciejowska, W. Nitka, T. Weron, Day-ahead vs. Intraday—Forecasting the price spread to maximize economic benefits, Energies 12 (4) (2019) http://dx.doi.org/10.3390/en12040631.

[15] F. Ocker, V. Jaenisch, The way towards European electricity intraday auctions–status quo and future developments, Energy Policy 145 (2020) 111731, http://dx.doi.org/10.1016/j.enpol.2020.111731.
[16] OpenWeather, One Call API, 2011, https://openweathermap.org/api/one-call-api. (Accessed on 30 January 2011).
[17] E. Perez, H. Beltran, N. Aparicio, P. Rodriguez, Predictive power control for PV plants with energy storage, IEEE Trans. Sustain. Energy 4 (2) (2012) 482–490, http://dx.doi.org/10.1109/TSTE.2012.2210255.
[18] M. Raugei, E. Leccisi, V.M. Fthenakis, What are the energy and environmental impacts of adding battery storage to photovoltaics? A generalized life cycle assessment, Energy Technol. 8 (11) (2020) 1901146, http://dx.doi.org/10.1002/ente.201901146.
[19] REN21, Renewables 2022 global status report, Paris: REN21 Secretariat, Paris, 2022.
[20] M. Shafie-khah, E. Heydarian-Forushani, M.E.H. Golshan, M.P. Moghaddam, M.K. Sheikh-El-Eslami, J.P. Catalao, Strategic offering for a price-maker wind power producer in oligopoly markets considering demand response exchange, IEEE Trans. Ind. Inform. 11 (6) (2015) 1542–1553, http://dx.doi.org/10.1109/TII.2015.2472339.
[21] S. Teleke, M.E. Baran, S. Bhattacharya, A.Q. Huang, Optimal control of battery energy storage for wind farm dispatching, IEEE Trans. Energy Convers. 25 (3) (2010) 787–794, http://dx.doi.org/10.1109/TEC.2010.2041550.
[22] S. Teleke, M.E. Baran, A.Q. Huang, S. Bhattacharya, L. Anderson, Control strategies for battery energy storage for wind farm dispatching, IEEE Trans. Energy Convers. 24 (3) (2009) 725–732, http://dx.doi.org/10.1109/TEC.2009.2016000.
[23] X. Wang, D.M. Vilathgamuwa, S. Choi, Determination of battery storage capacity in energy buffer for wind farm, IEEE Trans. Energy Convers. 23 (3) (2008) 868–878, http://dx.doi.org/10.1109/TEC.2008.921556.
[24] T. Wen, Z. Zhang, X. Lin, Z. Li, C. Chen, Z. Wang, Research on modeling and the operation strategy of a hydrogen-battery hybrid energy storage system for flexible wind farm grid-connection, IEEE Access 8 (2020) 79347–79356, http://dx.doi.org/10.1109/ACCESS.2020.2990581.
[25] J. Yang, M. Yang, M. Wang, P. Du, Y. Yu, A deep reinforcement learning method for managing wind farm uncertainties through energy storage system control and external reserve purchasing, Int. J. Electr. Power Energy Syst. 119 (2020) 105928, http://dx.doi.org/10.1016/j.ijepes.2020.105928.
[26] C. Zhang, H. Cheng, L. Liu, H. Zhang, X. Zhang, G. Li, Coordination planning of wind farm, energy storage and transmission network with high-penetration renewable energy, Int. J. Electr. Power Energy Syst. 120 (2020) 105944, http://dx.doi.org/10.1016/j.ijepes.2020.105944.
[27] Z. Zhang, Y. Zhang, Q. Huang, W.-J. Lee, Market-oriented optimal dispatching strategy for a wind farm with a multiple stage hybrid energy storage system, CSEE J. Power Energy Syst. 4 (4) (2018) 417–424, http://dx.doi.org/10.17775/CSEEJPES.2018.00130.